Delayed ^{18}F-FDG PET for Detection of Paraaortic Lymph Node Metastases in Cervical Cancer Patients

Shih-Ya Ma, MD[1]; Lai-Chu See, PhD[2]; Chyong-Huey Lai, MD[3]; Hung-Hsueh Chou, MD[3]; Chien-Sheng Tsai, MD[4]; Koon-Kwan Ng, MD[5]; Swei Hsueh, MD[6]; Wuu-Jyh Lin, PhD[7]; Jenn-Tzong Chen, MSc[7]; and Tzu-Chen Yen, MD, PhD[1]

[1]Department of Nuclear Medicine, Chang Gung Memorial Hospital and Chang Gung University, Taoyuan, Taiwan; [2]Biostatistics Consulting Center, Department of Public Health, Chang Gung University, Taoyuan, Taiwan; [3]Division of Gynecologic Oncology, Department of Obstetrics and Gynecology, Chang Gung Memorial Hospital and Chang Gung University, Taoyuan, Taiwan; [4]Department of Radiation Oncology, Chang Gung Memorial Hospital and Chang Gung University, Taoyuan, Taiwan; [5]Department of Radiology, Chang Gung Memorial Hospital and Chang Gung University, Taoyuan, Taiwan; [6]Department of Pathology, Chang Gung Memorial Hospital and Chang Gung University, Taoyuan, Taiwan; and [7]Institute of Nuclear Energy Research, Taoyuan, Taiwan

This prospective study investigated the usefulness of dual-phase ^{18}F-FDG PET scans (40 min and 3 h) in detecting paraaortic lymph node (PALN) metastasis for cervical cancer. **Methods:** One hundred four consecutive cervical cancer patients (International Federation of Gynecology and Obstetrics staging Ib–IVb, recurrent or persistent tumors) were included. All patients received a whole-body ^{18}F-FDG PET scan at 40 min and an additional scan from the T11 level to the inguinal region at 3 h after injection of 370 MBq ^{18}F-FDG. The maximum standardized uptake value (SUV) and retention index (RI [%], obtained by subtracting the normalized SUV value obtained at 40 min from that at 3 h) of the lesions were determined. **Results:** In all, 38 of the 104 patients were confirmed to have PALN metastases. For 31 patients (81.6%) with 13 upper (L1–L2 level) and 30 lower (L3–L4 level) PALNs, these metastases were detected with the 40-min scan. In addition, for 7 patients (18.4%) with 7 lower PALNs, metastases were found with the 3-h scan (RI = 12.6%). Two patients (3.0%) had 2 false-positive lesions initially (40 min) but were classified as benign with the 3-h scan. The sensitivity, specificity, and accuracy of ^{18}F-FDG PET scans at 40 min were 81.6%, 97.0%, and 91.3%, respectively. These quantities were all 100% when both the 40-min and 3-h scans were taken together. Eight patients (21.1%) had their treatment planning changed. We divided the 38 patients into 2 subgroups. Subgroup A included those with either only upper or only lower PALN metastases, and subgroup B included those with both upper and lower PALN metastases. In subgroup A, the SUV values were greater in the upper than in the lower PALNs in both the 40-min and 3-h images ($P = 0.077$). In subgroup B, there was no significant difference of SUV values between upper and lower PALNs in the 40-min ($P = 0.433$) and 3-h ($P = 0.937$) images. **Conclusion:** Our results showed that an additional 3-h scan is helpful for PALN detection of cervical cancer patients. A delayed image (3 h) is especially useful for lower PALN metastases.

Key Words: delayed ^{18}F-FDG PET; paraaortic lymph nodes; cervical cancer

Cervical carcinoma is the most common gynecologic malignancy in Taiwan. Factors that affect prognosis include the stage, status of the lymph nodes (LNs), and size and histologic grade of the primary tumor (*1–3*), of which the status of the paraaortic lymph nodes (PALNs) is the most important (*1,2,4*). Definitive irradiation is the mainstay of treatment for patients with locally advanced disease, such as PALN metastasis (*5–10*). In the past, MRI and CT scans have been used as noninvasive imaging to detect LN involvement in cervical cancer but were not entirely satisfactory. The reason may be due not only to tumors that exhibit high signal intensity on T2-weighted images but also to the inflammation and edema associated with acute radiation change (which may persist for up to 18 mo) or scar tissue due to postoperative or radiation-induced changes that also demonstrate high signal intensity on T2-weighted images (*11–13*). Although surgical staging is the most accurate method for identification of PALNs, this procedure may increase the complication rate (*7,8*). Thus, a useful, noninvasive method to evaluate the status of PALNs is needed.

The ^{18}F-FDG PET scan has been used for detection of some tumors, including cervical cancer. A positive scan results from detection of increased tumor cell glucose metabolism (*14–21*). Although malignant lesions may have higher levels of standardized uptake value (SUV), various

benign conditions, such as inflammation cells or granulation tissue, may also have a high SUV (22–24). Owing to the longer time required for levels of ^{18}F-FDG to plateau in cancer cells, than in inflammatory cells in cell line studies, some investigators performed delayed ^{18}F-FDG PET imaging to differentiate benign from malignant lesions in various cancers. The results showed that this delayed scan is valuable (25–31).

Although some studies showed that the ^{18}F-FDG PET scan was useful in cervical cancer (18–20), to the best of our knowledge, no one has used an additional 3-h image to evaluate the value of the ^{18}F-FDG PET scan in PALN detection. We thus designed this study to further understanding of the value of delayed imaging at 3 h, especially focusing on the value of PALN detection in cervical cancer.

MATERIALS AND METHODS

Patients

This study was approved by the institutional review board of Chang Gung Memorial Hospital. Written informed consent was obtained from all patients. Eligibility criteria were (a) histologic diagnosis of epithelial cervical carcinoma (including the histologic types of squamous cell carcinoma, adenocarcinoma, adenosquamous carcinoma, small cell carcinoma, and poorly differentiated carcinoma); (b) willingness to receive a CT- or ultrasound-guided biopsy or surgical exploration if indicated; (c) pelvic MRI and abdominal MRI or CT scanning was performed in all patients with previously untreated lesions and scheduled for radiotherapy or surgery with curative intent, with at least 1 enlarged pelvic LN (maximum dimension ≥ 1.0 cm); (d) histologically proven recurrent or persistent cancer after definitive radiotherapy or surgery and willing to receive salvage therapy of curative intent; (e) unexplained squamous cell carcinoma antigen (SCC-Ag) or carcinoembryonic antigen (CEA) elevation (SCC-Ag > 2 ng/mL or CEA > 10 ng/mL on 2 tests, 1 mo apart) at 6 mo after previous definitive treatment; (f) had completed curative salvage treatment with reelevation of tumor markers (criteria as above) or with untreated sites, which appear equivocal, in a pretreatment ^{18}F-FDG PET scan 3–6 mo after salvage therapy. An abdominal CT or MRI scan and pelvic MRI studies were done within 1 wk of the ^{18}F-FDG PET scan. A ^{18}F-FDG PET scan and an abdominal and pelvic CT or MRI scan were obtained on all patients within the 2 wk before the operation or biopsy.

CT

All CT images were obtained by a Hi-Speed CT scanner (General Electric Medical Systems) or a Somatom Plus 4 multislice CT scanner (Volume Zone, Version A40; Siemens AG Medical). All patients were required to fast for at least 4 h before the study, and they received a bowel preparation with oral meglumine diatrizoate (Gastrografin; Schering Health Care). An adequate intravenous route for an 18-gauge infusion set was prepared and hyoscine-N-butylbromide (40 mg) was injected intravenously to reduce bowel loop peristalsis, if necessary. Scanning was done in the craniocaudal direction, between the upper neck region and the symphysis pubis. Contrast enhancement with 100 mL iopomide (Ultravist 300; Schering Health Care) was used if necessary. Using the Hi-Speed CT scanner, contiguous slices of 5-mm thickness were obtained for the pelvis and abdomen. With the Somatom Plus 4

multislice CT scanner, contiguous slices of 10-mm thickness were obtained for the pelvis and abdomen.

MRI

All MR images were obtained by performing different pulse sequences with either a 1.5-T Magnetom Vision or a Magnetom Expert Scanner (Siemens Medical Systems). A phased-array body coil with a 50-cm transverse field of view was used. For pelvis and abdomen, transaxial, sagittal, and coronal sections with T2 spin-echo (repetition time/echo time [TR/TE], 4,000/99) and T1 spin-echo (TR/TE, 500/15) sequences were obtained. For chest and neck, transaxial, sagittal, and coronal sections with T2 spin-echo (TR/TE, 4,000/150) were acquired. The matrix size was 256×256 pixels. The slice thickness in the transaxial plane was 5 mm and in the sagittal and coronal planes in the pelvis and abdomen the slice thickness was 2.5 mm. As for chest and neck LN searches, the slice thickness was 7 mm in the transaxial plane and 6 mm in the sagittal and coronal planes.

^{18}F-FDG PET

A whole-body ^{18}F-FDG PET scan was obtained using an ECAT HR+ scanner. After the patient fasted for 6 h, 370 MBq (370 mCi) ^{18}F-FDG was administrated intravenously. Serum glucose levels were obtained immediately before the ^{18}F-FDG injection. Sedation with 2 mg of valium orally was given just before the ^{18}F-FDG injection to decrease muscular uptake. Scanning from the vertex to the upper thighs was performed in all patients at 40 min after injection. An additional 3-h scan was obtained in all subjects from T11 to the inguinal region. Transmission scans were obtained with ^{68}Ge rod sources. Reconstruction of both transmission and emission scans used accelerated maximum likelihood reconstruction and ordered-subset expectation maximization, which reduces image noise and avoids reconstruction artifacts resulting from filtered backprojection reconstruction of data with low count densities. To reduce urinary tract artifactual activity, a Foley catheter was placed before administration of ^{18}F-FDG. Additionally, all patients received intravenous hydration and a diuretic (intravenous furosemide, 20 mg) immediately before ^{18}F-FDG PET data acquisition at 40 min.

For semiquantitative analysis, the SUVs were obtained by placing regions of interest (ROIs) around the lesions that had previously been identified as suspicious on visual analysis. To minimize partial-volume effects, the maximum SUV within an ROI was used. The SUV was calculated as follows: SUV = (decay-corrected activity [kBq] per milliliter of tissue volume)/(injected ^{18}F-FDG activity [kBq]/body mass [g]). The retention index (RI) was (SUV2 − SUV1)/(SUV1), where SUV1 and SUV2 are the values of SUV at 40 min and 3 h, respectively. RI is usually expressed as a percentage.

Image Interpretation

MR or CT images were analyzed at 3 independent time points by an experienced radiologist with no knowledge of the PET results. The interpretation was made visually using a 5-point grading system (0 = completely normal finding; 1 = visible LNs, which were <0.5 cm in maximum dimension and considered reactive and unrelated to metastasis; 2 = if any single visible LN between 0.5 and 1 cm was seen; 3 = LNs of >1 cm in length in the short axis or multiple LNs (>3) between 0.5 and 1 cm; and 4 = confluent LNs with central necrosis or an irregular contour). Three experienced nuclear physicians, who were unaware of other imaging results and the clinical data, analyzed the PET images using

an interactive computer display. Any foci of increased ^{18}F-FDG uptake were also interpreted visually using a 5-point grading system (0 = negative finding; 1 = insignificant, yet visible lesion; 2 = equivocal, needs further follow-up and evaluation; 3 = probably metastasis; and 4 = significant metastasis). The ^{18}F-FDG PET scan was mainly interpreted visually. When a scoring decision could not be easily made by only visual analysis (i.e., low ^{18}F-FDG uptake lesion), we used the SUV and RI as additional criteria. In the 40-min scan only, for an equivocal visually interpreted lesion (score = 2) with an SUV1 value of ≥ 3, the score became 3. When 40-min and 3-h scans were taking together, a lesion would be interpreted as malignant (score 3 or 4) if the RI was more than -10%. The official ^{18}F-FDG PET report was used for this analysis.

Evaluation of ^{18}F-FDG PET Scan and CT or MRI Results

The gold standard for PALN metastasis was (a) it was pathologically proven through CT-guided biopsy or surgical exploration, (b) ^{18}F-FDG PET and CT or MR images had a concordant positive finding, or (c) a positive finding was found on the follow-up image studies. True-positive (TP) was defined as those with PALN metastasis and either ^{18}F-FDG PET scan or CT or MRI scan positive. True-negative (TN) was defined as those without PALN metastasis and with both ^{18}F-FDG PET and CT or MRI scans negative and the patient disease free for at least 6 mo afterward, with clinical and imaging follow-up. False-positive (FP) was counted for those without PALN metastasis and with either ^{18}F-FDG PET scan or CT or MRI scan positive. False-negative (FN) was for those with PALN metastasis and either ^{18}F-FDG PET scan or CT or MRI scan negative.

Statistical Analysis

The Wilcoxon rank sum test or Wilcoxon signed rank test was used to assess the differences between upper or lower PALNs of SUVs at 40 min and at 3 h and RI. Such differences were considered for those patients with either upper or lower PALNs (but not both upper and lower) and separately for those with both upper and lower PALNs. Scatter plots and Pearson correlation coefficients allowed the relationship between SUV at 40 min and at 3 h to be explored. Simple linear regression was conducted to obtain a predictive equation of SUV at 3 h using SUV at 40 min as a predictor for those with either upper or lower PALNs. For those with both upper and lower PALNs, a generalized estimating equation (GEE) was used to obtain a predictive equation for SUV at 3 h using the SUV at 40 min as a predictor and to examine the adjusted difference in SUV at 3 h between upper and lower PALNs (*32*). The SAS win/8.12 package was used to perform the statistical analysis. A 2-tailed value of $P < 0.05$ was considered significant.

RESULTS

From February 2001 to February 2003, 104 consecutive cervical cancer patients (International Federation of Gynecology and Obstetrics [FIGO] staging Ib–IVb, recurrence and persistent tumor) were enrolled (age range, 25–86 y; mean $\pm$ SD, 53.7 $\pm$ 12.0 y). The following types of histopathology were found in these patients: squamous cell carcinoma in 84, adenocarcinoma in 9, adenosquamous cell carcinoma in 5, small cell carcinoma in 4, and poorly differentiated carcinoma in 2. Thirty-nine had an initial diagnosis of cervical cancer (FIGO staging of Ib in 14, IIa in 2, IIb in 12, IIIa in 0, IIIb in 4, IVa in 1, and IVb in 6) (group I). The other 65 patients had recurrence at 1 site ($n = 31$) or at 2 sites ($n = 21$) (group II) or had unexplained elevation of tumor markers (SCC-Ag > 2 ng/mL or CEA > 10 ng/mL on 2 tests, 1 mo apart) ($n = 13$) (group III).

Table 1 demonstrates the results of PALN detection with dual-phase ^{18}F-FDG PET scans. The criteria we used in this study for TP in a ^{18}F-FDG PET scan were a visual score of ≥ 3, with or without reference to SUV and RI (SUV1 ≥ 3 or SUV1 < 3 but with RI more than -10%). In all, 50 lesions from 38 patients were found on ^{18}F-FDG PET scans. Forty lesions had SUV1 ≥ 3 initially and 10 lesions were those with SUV1 < 3 and RI of more than -10%. All 38 patients had PALN metastases. Of them, the diagnoses in 11 patients were confirmed histologically via CT-guided biopsy ($n = 9$) or surgical exploration ($n = 2$), and 19 patients had concordant positive findings in both ^{18}F-FDG PET and CT or MR images. In the remaining 8 patients, the diagnoses were further confirmed by a second CT or MRI follow-up. Sixteen patients (41.0%) were from primary cervical cancer (group I). Nineteen patients (36.5%) were from documented recurrent cervical cancer with potentially curative intent (group II). Three patients (23.1%) were from unexplained elevation of tumor markers (group III). Among these 38 patients, the disease was detected in 31 with a 40-min scan (81.6%). Thirteen patients (33.3%) were group I, 16 patients (30.8%) were group II, and 2 patients (15.4%) were group III. An additional 7 PALNs (18.4%) were found when the 40-min and 3-h scans were carefully compared (FN in the 40-min scan became TP after 3-h scans) (Fig. 1). Three patients (7.7%) were group I, 3 patients (5.8%) were group II, and 1 patient (7.7%) was group III. Two patients were FP after the 40-min scan (3.0%) and became TN after considering both the 40-min and 3-h scans (Fig. 2). One was group II and the other was group III. Eight patients (21.1%) had their treatment planning changed after the 3-h scan. Four were group I, 1 was group II, and the others were group III (3 patients with FN in 40 min and TP in 3 h: 2 were group I and 1 was group III). Table 2 demonstrates the results of patient-based PALN detection with CT or MRI and ^{18}F-FDG PET at 40 min only and at 40 min and 3 h. In comparison with the final results, the sensitivity, specificity, positive predictive value (PPV), negative predictive value (NPV), and accuracy for CT or MRI were 76.3%, 97.0%, 93.5%, 87.7%, and 89.4%. For the ^{18}F-FDG PET scan at 40 min only, the above quantities were 81.6%, 97.0%, 93.9%, 90.1%, and 91.3%, respectively. These parameters were all equal to 100% when ^{18}F-FDG PET scans at both 40 min and 3 h were considered. Two patients (3.0%) were recognized as FP in CT or MR images, and all were TN from the 40-min ^{18}F-FDG PET scan. For the 2 FP findings found in CT or MRI scans, 1 was due to postirradiation changes and the other resulted from small tortuous vessels in the paraaortic region. Nine patients (23.7%) were considered to have

TABLE 1
Results of PALN Detection with ^{18}F-FDG PET Scans Obtained at 40 Minutes Only and at Both 40 Minutes and 3 Hours

Patient no.	Group	Upper 40 min	Upper 40 min and 3 h	Lower 40 min	Lower 40 min and 3 h	R/T[†]	SUV1	SUV2	RI (%)	Final[‡]
1	I	0	0	3	4	No	3.28	4.16	26.83	A
2	I	0	0	3	4	No	3.17	3.11	−1.89	B
3	II	3	4			No	3.69	3.62	−1.90	B
				4	4		5.52	6.17	11.78	
4	II	0	0	4	4	Pelvis	6.76	7.74	14.50	B
5	II	0	0	4	4	No	8.70	9.38	7.82	A
6	II	3	4			Pelvis	2.65	3.06	15.47	A
				3	4		2.16	2.46	13.89	
7	III	0	0	4	4	Pelvis	4.46	6.19	38.79	C
8	II	0	0	4	4	L-1/2	4.44	8.08	81.98	A
9	I	0	0	3	4	No	3.22	6.14	90.68	C
10	I	4	4			No	5.12	6.85	33.79	B
				3	4		2.76	3.92	42.03	
11	II	0	0	3	4	Pelvis	3.39	3.41	0.59	B
12	I	0	0	4	4	No	5.74	5.84	1.74	B
13	II	4	4			Pelvis	7.20	8.98	24.72	A
				4	4		5.54	4.35	−21.48	
14	II	4	4			No	7.12	7.34	3.09	B
				4	4		7.84	7.28	−7.14	
15	II	4	4			L-1/2	11.4	10.65	−6.58	B
				4	4		4.53	4.05	−10.6	
16	I	0	0	3	4	No	3.96	4.89	23.48	B
17	I	4	4			No	8.43	8.82	4.63	B
				4	4		4.34	4.41	1.61	
18	II	0	0	4	4	Pelvis	5.60	4.57	−18.39	B
19	I	0	0	4	4	No	10.58	9.54	−9.83	B
20	II	4	4			Pelvis	6.10	6.31	3.44	A
				4	4		10.30	9.16	−11.07	
21	II	4	4	0	0	L-3/4	11.14	11.05	−0.81	B
22	I	0	0	3	4	No	3.90	5.38	37.95	B
23	II	0	0	3	4	Pelvis	3.60	4.50	25.00	B
24	I	4	4			No	6.82	5.66	−17.01	B
				4	4		11.03	9.54	−13.51	
25	I	0	0	4	4	No	7.07	5.49	−22.35	C
26	II	0	0	3	4	Pelvis	3.7	4.5	21.62	A
27	II	0	0	4	4	Pelvis	9.52	6.52	−31.51	A
28	I	4	4			No	10.3	12.08	17.28	B
				4	4		12.56	14.25	13.46	
29	II	4	4			Pelvis	4.28	3.02	−29.44	A
				4	4		7.1	7.6	7.04	
30	III	0	0	4	4	L-1/2	5.86	5.41	−7.68	C
31	I	3	4			No	3.59	5.41	50.70	B
				4	4		13.08	16.01	22.40	
32	II	0	0	2	3	L-1/2	2.39	2.34	−2.09	A
33	I	0	0	2	3	No	2.49	3.37	35.34	C
34	II	0	0	2	3	Pelvis	2.84	3.03	6.69	A
35	II	0	0	2	3	Pelvis	2.18	2.85	30.73	C
36	I	0	0	2	3	No	1.85	1.79	−3.24	C
37	III	0	0	2	3	No	1.88	2.03	7.98	C
38	I	0	0	2	3	No	2.09	2.35	12.44	B
Mean ± SD							5.75 ± 3.11	6.09 ± 3.17	10.26 ± 24.58	

*Grades are 0 = normal; 1 = insignificant visible lesion; 2 = equivocal, needs further follow-up and evaluation; 3 = probably metastasis; and 4 = significant metastasis.

[†]In R/T (radiation therapy), No = never treated before, Pelvis = radiation field was confined to pelvis, and L-3/4 or L-1/2 = radiation field was applied up to level of L3 or L1.

[‡]A = pathologically proven, B = concordant positive findings of ^{18}F-FDG PET and CT or MR images, and C = confirmed by second CT or MRI follow-up.
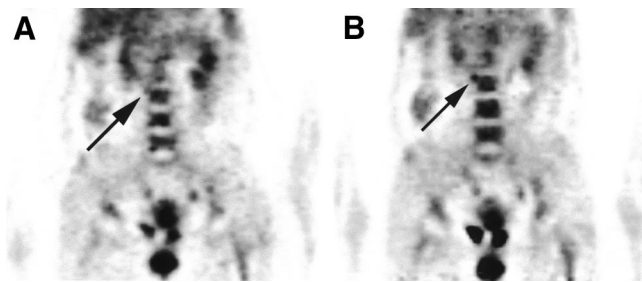
FIGURE 1. A 52-y-old woman with cervical cancer stage IVb. (A) ^{18}F-FDG PET scan reveals focal area of slightly increased ^{18}F-FDG-6-phosphate accumulation in right lower PALN (arrow; SUV = 2.49; score 2) in 40-min PET scan. (B) In 3-h scan, lesion is more clearly evident (arrow; SUV = 3.37, RI = 35.34%; score 3).

FN CT or MR images. Among them, 5 (55.6%) were TP with the 40-min ^{18}F-FDG PET scan only and 4 (44.4%) were TP with both the 40-min and 3-h ^{18}F-FDG PET scans. Three of them were visible LNs of 0.5–1 cm in maximum dimension and the others were <0.5 cm.

Because there was a worse prognosis for upper PALN metastases than for lower PALN metastases in cervical cancer patients (*8*), we divided the PALNs into those in the upper (L1–L2) and lower (L3–L4) levels. Table 3 illustrates the results of upper and lower PALN detection at 40 min only and at 40 min and 3 h. For the 50 lesions detected in 38 patients this study, 43 (86%) were detected in the 40-min scan (SUV1 = 6.32 ± 2.99 and SUV2 = 6.67 ± 3.04), with 13 upper and 30 lower PALNs. An additional 7 lesions (14%) were detected when both the 40-min and 3-h scans were considered (SUV1 = 2.25 ± 0.35 and SUV2 = 2.54 ± 0.57; RI range = -2.09% to 35.34%). All 7 lesions were lower PALNs. In comparison, the SUV2 (6.09 ± 3.17) was higher than the SUV1 (5.75 ± 3.11) ($P = 0.054$), indicating increasing ^{18}F-FDG-6-phosphate uptake with time in malignant lesions. With the additional information from the RI, 2 FP findings in the 40-min ^{18}F-FDG PET study (SUV1 = 6.96 for a lower PALN in patient 1 and 2.43 for an upper PALN in patient 2) became TN in the 40-min and 3-h scan (with negative findings for both patients 1 and 2).

For further understanding of the ^{18}F-FDG uptake in those with either PALN metastases at upper or lower levels and those with both upper and lower PALNs metastases, we divided these 38 patients into 2 groups, subgroups A and B. Subgroup A comprised those with either upper or lower PALNs and subgroup B included those with both upper and lower PALNs. In subgroup A, the SUVs for upper PALNs' SUVs were greater (with minimal significance) than those for lower PALNs only, in both the 40-min (11.14 vs. 4.51 ± 2.42, $P = 0.077$) and the 3-h (11.05 vs. 4.90 ± 2.19, $P = 0.077$) scans (Table 4), although there was only 1 patient with upper PALNs. In subgroup B, no significant difference in SUVs in upper and lower nodal uptake on either 40-min

(6.39 ± 2.72 vs. 7.23 ± 3.74) or 3-h (6.81 ± 2.92 vs. 7.43 ± 4.22) images ($P = 0.433$ vs. $P = 0.937$) was seen (Table 5). There was also no significant difference in RI between upper and lower PALNs in subgroup B.

Figures 3 and 4 plot SUVs at 40 min versus 3 h for subgroups A and B, respectively. Both demonstrate a significant positive correlation between the SUVs at 40 min and 3 h ($r = 0.942$, $P < 0.001$ for subgroup A; $r = 0.942$, $P < 0.001$ for subgroup B). In subgroup A, the predictive equation obtained from simple linear regression is SUV at 3 h = $1.35 + (0.80 \times$ SUV at 40 min). In subgroup B, the predictive equation obtained from a GEE is SUV at 3 h = $-0.01 + (1.07 \times$ SUV at 40 min) for upper PALNs and SUV at 3 h = $-0.29 + (1.07 \times$ SUV at 40 min) for lower PALNs. There is no difference in the SUV at 3 h between upper and lower PALNs after the SUV at 40 min was adjusted ($P = 0.393$).

DISCUSSION

Detection of PALN metastases is important for cervical cancer patients because the prognosis is significantly worse if there is a PALN metastasis. Once PALNs are identified, treatment planning for such patients should be more aggressive (*5–10*). According to the literature, the incidence of PALN metastases in cervical cancer patients varies from 4.3% to 25% (*3,5,8,11,18,33,34*). With progress in treatment planning, earlier and more precise detection of PALN metastases may improve the survival rate.

A CT or MRI scan is frequently obtained for metastatic LN detection in cervical cancer. The diagnosis of nodal abnormality in a CT or MRI scan is based on size and morphology. However, because of difficulty in differentiating nodal metastasis from inflammatory adenopathy and fibrotic change, the sensitivity and specificity for metastatic LN detection in CT and MRI is suboptimal, especially for those who previously received radiation therapy (*11–13*). With ^{18}F-FDG PET imaging of cancer cells, the abnormality detected is increased uptake, reflecting increased glucose metabolism in the tumor cell, rather than any abnormal morphology and increased size.
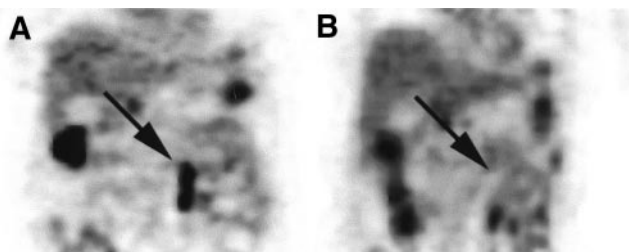
FIGURE 2. A 74-y-old woman had previously treated cervical cancer with unexplained elevated SCC-Ag tumor marker. (A) ^{18}F-FDG PET scan shows increased ^{18}F-FDG-6-phosphate accumulation in left lower PALNs in 40-min scan (arrow; SUV = 6.96; score 4). (B) In 3-h scan, previous lesion is not well demonstrated (arrow).

TABLE 2
PALN Detection Results After ^{18}F-FDG PET (at 40 Minutes Only and After Imaging at Both 40 Minutes and 3 Hours) and CT or MRI

Imaging modality	TP	TN	FP	FN	Sensitivity (%) [95% CI]	Specificity (%) [95% CI]	PPV (%) [95% CI]	NPV (%) [95% CI]	Accuracy (%) [95% CI]
^{18}F-FDG PET									
40-min scan only	31	64	2	7	81.6 [65.7–92.3]	97.0 [89.5–99.6]	93.9 [79.8–99.3]	90.1 [80.7–95.9]	91.3 [84.2–96.0]
Both 40-min and 3-h scans	38	66	0	0	100.0	100.0	100.0	100.0	100.0
CT or MRI	29	64	2	9	76.3 [59.8–88.6]	97.0 [89.5–99.6]	93.5 [78.6–99.2]	87.7 [77.9–94.2]	89.4 [81.9–94.6]

CI = confidence interval.

The ^{18}F-FDG PET scan has been shown to be useful in detection of primary tumor and metastatic lesions for cervical and several other cancers, although some FP findings have been reported (14–21). Also, the SUV has been widely accepted as a semiquantitative method for analysis of ^{18}F-FDG PET scans because of its positive correlation with glucose utilization in cancer cells (35–37). However, many studies showed that the SUV had some limitations in differentiating benign from malignant lesions. For example, various conditions, such as inflammatory processes, granulation tissue, and so forth, may initially exhibit significantly high SUV values due to overexpression of glucose transporter (22–24). Thus, if we use a standard protocol (i.e., a ^{18}F-FDG PET scan started at 40 min after ^{18}F-FDG injection), this may result in FP or FN findings. Because of overexpression of hexokinase and underexpression of glucose-6-phosphatase activities in cancer cells, but not in inflammatory cells or granulation tissues, some investigators used dual-time or delayed ^{18}F-FDG PET scans to differentiate benign from malignant lesions (25–31). The re-

sults of such studies showed that most of the SUV values in malignant lesions were increased in the delayed scan and for most benign lesions these delayed values decreased. In this study, the SUV2 (6.09 ± 3.17) was slightly but not significantly higher than the SUV1 (5.75 ± 3.11) (P = 0.054). With the 40-min and 3-h scans, 7 additional PALN metastases (18.4%) were detected and 2 (3.0%) became TN. The sensitivity, specificity, PPV, NPV, and accuracy for PALN detection in this study using CT or MRI scans were 76.3%, 97.0%, 93.5%, 87.7%, and 89.4%, respectively. Although ^{18}F-FDG PET at 40 min (81.6%, 97.0%, 93.9%, 90.1%, and 91.3% for these quantities) was better than CT or MRI for such detection, ^{18}F-FDG PET at both 40 min and 3 h was more significant, with values of 100% for each of these 5 quantities. Even though the gold standard of lesion detection was pathologically proven or appropriate clinical and second imaging follow-up, some microscopic and indolent PALN metastatic lesions might be missed by all imaging modalities. Therefore, it is possible that the results of PALN detection with CT or MRI and dual-

TABLE 3
Upper and Lower PALN Detection After ^{18}F-FDG PET (at 40 Minutes Only and After Imaging at Both 40 Minutes and 3 Hours)

^{18}F-FDG PET scan timing	TP	TN	FP	FN	Sensitivity (%) [95% CI]	Specificity (%) [95% CI]	PPV (%) [95% CI]	NPV (%) [95% CI]	Accuracy (%) [95% CI]
40-min scan only									
Upper	13	90	1	0	100 —	98.9 [94.0–99.9]	92.9 [66.1–99.8]	100 —	99 [94.8–99.9]
Lower	30	66	1	7	81.1 [64.8–92.0]	98.5 [92.0–99.9]	96.8 [83.3–99.9]	90.4 [81.2–96.1]	92.3 [85.4–96.6]
Both 40-min and 3-h scans									
Upper	13	91	0	0	100.0	100.0	100.0	100.0	100.0
Lower	37	67	0	0	100.0	100.0	100.0	100.0	100.0
Total	50	158	0	0	100.0	100.0	100.0	100.0	100.0

CI = confidence interval.

TABLE 4
SUV and RI at 40 Minutes and 3 Hours in 26 Patients in Subgroup A with TP Findings for Either Upper or Lower PALNs

Parameter	Total ($n = 26$)	Upper only ($n = 1$)	Lower only ($n = 25$)	P value*
SUV at 40 min	4.76 ± 2.71	11.14	4.51 ± 2.42	0.077
SUV at 3 h	5.14 ± 2.45	11.05	4.90 ± 2.19	0.077
RI (%)	14.1 ± 28.2	−0.008	14.7 ± 28.6	0.692

*P values are from 1 Wilcoxon rank sum test.

FIGURE 3. Relation of SUVs between 40-min and 3-h scans for 26 TPs in either upper or lower PALNs (subgroup A). ■, upper PALN; ○, lower PALNs ($r = 0.942$, $P < 0.001$). Line plotted is SUV at 3 h = (1.35 + [0.80 × SUV at 40 min]).

phase ^{18}F-FDG PET in our study should be lower than presented in the Table 2.

The PALNs were located close to ureters, so ^{18}F-FDG-6-phosphate retention in the ureters may be misinterpreted as being PALN metastases. To overcome this, Foley catheter and urine irrigation were applied for all of our patients. Also, furosomide was administered to all patients. Uptake of ^{18}F-FDG-6-phosphate at the bowel was another difficulty in differentiating from PALNs metastases. Two initially FP PALNs were later deduced to be due to ^{18}F-FDG-6-phosphate uptake in the bowel. With a 3-h scan, they disappeared and were confirmed as TN.
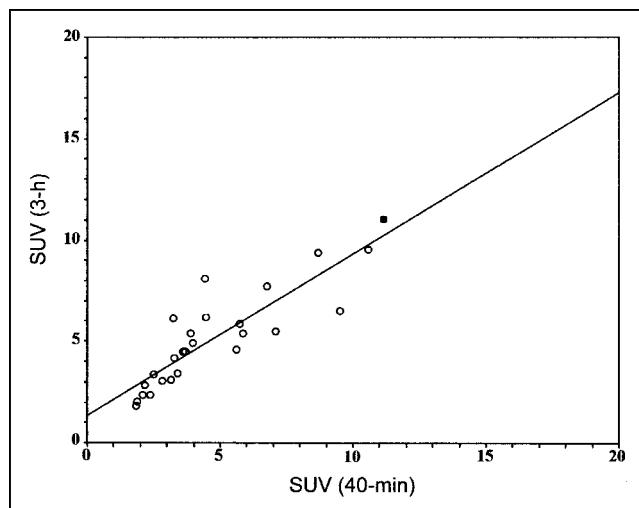
Extended field radiation therapy has been applied for the treatment of PALN metastases in cervical cancer patients. Thus, postirradiation changes in PALNs may confuse radiologists in their interpretation of lesions. Because ^{18}F-FDG-6-phosphate levels may increase in some benign conditions (i.e., causing a relatively high SUV1) but took longer to plateau in malignant cells than in benign lesions, an RI value of ≥10% was considered as a positive ^{18}F-FDG PET finding, especially after an equivocal or inconclusive ^{18}F-FDG PET scan at 40 min (or even at 60 min after injection) (25). In this study, we used either SUV1 of ≥3 or SUV1 of <3 but with RI of more than −10% as the additional criteria for a malignant lesion. We chose RI of more than −10% (rather than >10%) because of the otherwise missing 4 cases (10.5%). With these criteria, an additional 7 lower PALNs were found and no malignant lesion was missed. In comparison, ^{18}F-FDG PET scans were especially helpful in

detection of lower PALNs, more so with the use of scans at 40 min and at 3 h (100%) than with that at 40 min (81.6%) alone. With the additional information from ^{18}F-FDG PET at 40 min and 3 h, 8 patients (21.1%) had their treatment planning changed. For upper PALN metastasis only, there was just 1 such patient. In this case, the upper PALN lesions could be found both in 40-min and in 40-min and 3-h scans. Therefore, the value of dual-phase ^{18}F-FDG PET in detecting upper PALN metastases needs to be evaluated further.

TABLE 5
SUV and RI at 40 Minutes and 3 Hours in 12 Patients in Subgroup B with TP Findings for Both Upper and Lower PALNs

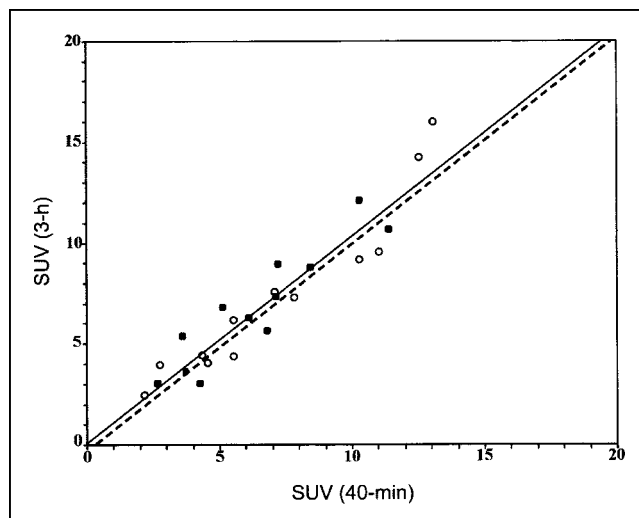| Parameter	Upper ($n = 12$)	Lower ($n = 12$)	P value*
SUV at 40 min	6.39 ± 2.72	7.23 ± 3.74	0.433
SUV at 3 h	6.81 ± 2.92	7.43 ± 4.22	0.937
RI (%)	8.2 ± 22.0	4.0 ± 18.0	0.388

*P values are from 1 Wilcoxon signed rank test.

FIGURE 4. Relation of SUVs between 40 min and 3 h for 12 TPs in both upper and lower PALNs (subgroup B). ■, lower PALNs; ○, upper PALNs ($r = 0.942$, $P < 0.001$). For upper PALNs, solid line plotted is SUV at 3 h = (−0.01 + [1.07 × SUV at 40 min]). For lower PALNs, dashed line plotted is SUV at 3 h = (−0.29 + [1.07 × SUV at 40 min]). There is no significant difference in SUV at 3 h between upper and lower PALNs, after SUV at 40 min was adjusted ($P = 0.393$).

Our study also showed that in those with either only upper or only lower PALN metastases, the former only had marginal significantly higher SUVs than the lower in both 40 min and 3 h ($P = 0.077$). These results may imply that the more malignant the cells' behavior, the more glucose they metabolize. Because there was only 1 patient having an upper PALN, further study is needed. For those patients with both upper and lower PALNs metastases, there was no significant difference between the SUVs in the upper and lower PALNs. These results may indicate that such metastases may share a common tumor biologic behavior.

Should an additional 3-h scan should be applied for all cervical cancer patients? To answer this question, we compared the results of the ^{18}F-FDG PET scans with the 38 PALN-positive cervical cancer patients. Our results showed that the ^{18}F-FDG PET at 3 h can detect more PALNs in group I than in groups II and III. Besides, for group I, the additional findings from ^{18}F-FDG PET at 3 h seemed to be helpful for clinicians in changing treatment planning. However, because of the limited number of patients included, more studies are warranted for a further understanding of which subgroup of cervical cancer patients should be highly recommended for both 40-min and 3-h ^{18}F-FDG PET scans.

Although information at 40 min and 3 h was valuable for PALN identification in our PET studies, 3-h information may be sometimes be inaccurate because of a position change in the PET table or misrecognition of ^{18}F-FDG accumulation in the ureter or bowel instead of an upper PALN. In such a condition, our equation of the SUV at 3 h predicted from the SUV at 40 min is helpful. According to the patients' PALN status (upper only, lower only, or both) and the 40-min SUV, it is easy to obtain the predicted 3-h SUV from our equation. The predicted 3-h SUV can help in judging the lesion status.

CONCLUSION

This prospective study showed that dual time point ^{18}F-FDG PET scans are important for metastatic PALN detection, especially for those located at the lower (L3 and L4) levels. Additional information using an RI of more than -10% aids in differentiating benign lesions from malignant PALNs, especially for those with SUV1 of <3. When there is a clinical suspicion of PALN metastases and curative intent in subsequent treatment of cervical cancer patients, a dual time point ^{18}F-FDG PET scan is recommended. We believe that these findings will be of practical value with the steadily increasing worldwide use of PET in oncology.

ACKNOWLEDGMENTS

REFERENCES

1. Hopkins MP, Morley GW. Prognostic factors in advanced stage squamous cell cancer of the cervix. *Cancer.* 1993;72:2389–2393.
2. Stehman FB, Bundy BN, DiSaia PJ, Keys HM, Larson JE, Fowler WC. Carcinoma of the cervix treated with radiation therapy. I. A multi-variate analysis of prognostic variables in the Gynecologic Oncology Group. *Cancer.* 1991;67:2776–2785.
3. Lai CH, Hong JH, Hsueh S, et al. Preoperative prognostic variables and impacts of postoperative adjuvant therapy in stage IB or II cervical carcinoma with or without pelvic node metastases: an analysis of 891 patients. *Cancer.* 1999;85:1537–1546.
4. Kim PY, Monk BJ, Chabra S, et al. Cervical cancer with paraaortic metastases: significance of residual paraaortic disease after surgical staging. *Gynecol Oncol.* 1998;69:243–247.
5. Lovecchio JL, Averette HE, Donato D, Bell J. 5-Year survival of patients with periaortic nodal metastases in clinical stage IB and IIA cervical carcinoma. *Gynecol Oncol.* 1989;34:43–45.
6. Stryker JA, Mortel R. Survival following extended field irradiation in carcinoma of cervix metastatic to para-aortic lymph nodes. *Gynecol Oncol.* 2000;79:399–405.
7. Rotman M, Pajak TF, Choi K, et al. Prophylactic extended-field irradiation of para-aortic lymph nodes in stages IIB and bulky IB and IIA cervical carcinomas: ten-year treatment results of RTOG 79-20. *JAMA.* 1995;274:387–393.
8. Vigliotti AP, Wen BC, Hussey DH, et al. Extended field irradiation for carcinoma of the uterine cervix with positive periaortic nodes. *Int J Radiat Oncol Biol Phys.* 1992;23:501–509.
9. Grigsby PW, Vest ML, Perez CA. Recurrent carcinoma of the cervix exclusively in the paraaortic nodes following radiation therapy. *Int J Radiat Oncol Biol Phys.* 1994;28:451–455.
10. Chou HH, Wang CC, Lai CH, et al. Isolated paraaortic lymph node recurrence after definitive irradiation for cervical carcinoma. *Int J Radiat Oncol Biol Phys.* 2002;51:442–448.
11. Heller PB, Maletano JH, Bundy BN, Barnhill DR, Okagaki T. Clinical-pathologic study of stage IIB, III, and IVA carcinoma of the cervix: extended diagnostic evaluation for paraaortic node metastasis—a Gynecologic Oncology Group study. *Gynecol Oncol.* 1990;38:425–430.
12. Hricak H, Yu KK. Radiology in invasive cervical cancer. *AJR.* 1996;167:1101–1108.
13. Subak LL, Hricak H, Powell CB, Azizi L, Stern JL. Cervical carcinoma: computed tomography and magnetic resonance imaging for preoperative staging. *Obstet Gynecol.* 1995;86:43–50.
14. Strauss LG, Conti PS. The applications of FDG PET in clinical oncology. *J Nucl Med.* 1991;32:623–648.
15. Delbeke D, Martin WH. Positron emission tomography imaging in oncology. *Radiol Clin North Am.* 2001;39:883–917.
16. Bar-Shalom R, Valdivia AY, Blaufox MD. FDG PET imaging in oncology. *Semin Nucl Med.* 2000;30:150–185.
17. McGuirt WF, Greven K, Williams D 3rd, et al. PET scanning in head and neck oncology: a review. *Head Neck.* 1998;20:208–215.
18. Rose PG, Adler LP, Rodriguez M, et al. Positron emission tomography for evaluating para-aortic nodal metastasis in locally advanced cervical cancer before surgical staging: a surgicopathologic study. *J Clin Oncol.* 1999;17:41–45.
19. Sugawara Y, Eisbruch A, Kosuda S, et al. Evaluation of FDG PET in patients with cervical cancer. *J Nucl Med.* 1999;40:1125–1131.
20. Grigsby PW, Siegel BA, Dehdashti F. Lymph node staging by positron emission tomography in patients with carcinoma of the cervix. *J Clin Oncol.* 2001;19:3745–3749.
21. Beggs D, Hain F, Curran M, O'Doherty J. FDG PET as a "metabolic biopsy" tool in non-lung lesions with indeterminate biopsy. *Eur J Nucl Med.* 2002;29:542–546.
22. Kapucu LO, Meltzer CC, Townsend DW, Keenan RJ, Luketich JD. Fluorine-18-fluorodeoxyglucose uptake in pneumonia. *J Nucl Med.* 1998;39:1267–1269.
23. Yamada S, Kubota K, Kubota R, Ido T, Tamahashi N. High accumulation of fluorine-18-fluorodeoxyglucose in turpentine-induced inflammatory tissue. *J Nucl Med.* 1995;36:1301–1306.
24. Dimitrakopoulou-Strauss A, Strauss LG, Heichel T, et al. The role of quantitative ^{18}F-FDG PET studies for the differentiation of malignant and benign bone lesions. *J Nucl Med.* 2002;43:510–518.
25. Higashi T, Saga T, Nakamoto Y, et al. Relationship between retention index in dual-phase ^{18}FDG PET, and hexokinase-II and glucose transporter-1 expression in pancreatic cancer. *J Nucl Med.* 2002;43:173–180.
26. Boerner AR, Weckesser M, Herzog H, et al. Optimal scan time for fluorine-18

fluorodeoxyglucose positron emission tomography in breast cancer. *Eur J Nucl Med.* 1999;26:226–230.

27. Hustinx R, Smith RJ, Benard F, et al. Dual time point fluorine-18 fluorodeoxyglucose positron emission tomography: a potential method to differentiate malignancy from inflammation and normal tissue in the head and neck. *Eur J Nucl Med.* 1999;26:1345–1348.

28. Nakamoto Y, Higashi T, Sakahara H, et al. Delayed ^{18}F-fluoro-2-deoxy-D-glucose positron emission tomography scan for differentiation between malignant and benign lesions in the pancreas. *Cancer.* 2000;89:2547–2554.

29. Zhuang H, Pourdehnad M, Lambright ES, et al. Dual time point ^{18}F-FDG PET imaging for differentiating malignant from inflammatory processes. *J Nucl Med.* 2001;42:1412–1417.

30. Matthies A, Hickeson M, Cuchiara A, Alavi A. Dual time point ^{18}F-FDG PET for the evaluation of pulmonary nodules. *J Nucl Med.* 2002;43:871–875.

31. Lodge MA, Lucas JD, Marsden PK, Cronin BF, O'Doherty MJ, Smith MA. A FDG PET study of [18]FDG uptake in soft tissue masses. *Eur J Nucl Med.* 1999;26:22–30.

32. Zeger SL, Liang KY. Longitudinal data analysis for discrete and continuous outcomes. *Biometrics.* 1986;42:121–130.

33. Possover M, Krause N, Kuhne-Heid R, Schneider A. Value of laparoscopic evaluation of paraaortic and pelvic lymph nodes for treatment of cervical cancer. *Am J Obstet Gynecol.* 1998;178:806–810.

34. Sakuragi N, Satoh C, Takeda N, et al. Incidence and distribution pattern of pelvic and paraaortic lymph node metastasis in patients with stages IB, IIA, and IIB cervical carcinoma treated with radical hysterectomy. *Cancer.* 1999;8:1547–1554.

35. Torizuka T, Tamaki N, Inokuma T, et al. In vivo assessment of glucose metabolism in hepatocellular carcinoma with FDG-PET. *J Nucl Med.* 1995;36:1811–1817.

36. Younes M, Brown RW, Stephenson M, Gondo M, Cagle PT. Over expression of Glut1 and Glut3 in stage I non small cell lung carcinoma is associated with poor survival. *Cancer.* 1997;80:1046–1051.

37. Higashi K, Ueda Y, Sakurai A, et al. Correlation of Glut1 glucose transporter expression with [^{18}F]FDG uptake in non-small cell lung carcinoma. *Eur J Nucl Med.* 2000;27:1778–1785.